

POST-PEAK BEHAVIOR OF FRP-JACKETED REINFORCED CONCRETE COLUMNS

Tidarut JIRAWATTANASOMKUL^{*1}, Dawei ZHANG^{*2} and Tamon UEDA^{*3}

ABSTRACT

The objective of this study is to propose a new analytical method considering the interaction of flexure and shear strengths in order to predict the post-peak responses of RC columns with and without FRP jacketing. This paper shows that the proposed analytical method can improve the prediction in the post-peak region by taking into account the confinement effect and the secant stiffness of reinforcement on the shear strength. The proposed analytical method shows a good agreement with the experimental database consisting of columns with and without FRP jacketing.

Keywords: post-peak, shear strength, secant stiffness, confinement, FRP jacketing

1. INTRODUCTION

Predicting the flexural and shear strength behavior of FRP-retrofitted columns has been a great challenge for seismic engineers due to the complicated interactions and significant nonlinear behavior of composite structures. In some design codes such as JSCE 2007 [2], this interconnection of flexural and shear strength behaviors is ignored. However, the previous researchers [1,2,3] have shown that flexural strength behavior influences shear strength behavior due to the yielding of the reinforcement. At the same time, shear strength behavior significantly affects flexural strength behavior in the reduction of the neutral axis depth. Furthermore, the reinforced concrete (RC) columns subjected to the seismic force with the high axial loading ratio are significantly influenced by this flexure-shear interaction behavior. However, several current shear strength model and design code [2,6] do not take into account this flexure-shear interaction.

It is evident that the post-peak behavior of these RC columns are dominated by the shear strength behavior [1,2,3] since the post-peak shear strength deteriorates due to the cracked concrete and yielding of reinforcement. Fig. 1 illustrates the conceptual failure modes of RC columns with interaction between flexural and shear strengths [1,2,3]. The relationship between applied shear force and deformation of these columns are indicated with flexural behavior and various conditions of shear strength (V_{su}). The intersection point between the flexural behavior and shear strength corresponds to the peak shear force and indicates the initiation of post-peak behavior. The failure mode can be distinguished by different cases of intersection point. Mode I corresponds to a brittle shear failure as the intersection point occurs before the flexural yielding (V_y). Following the flexural yielding, a column behaves as less ductile shear failure (Mode II) if the intersection

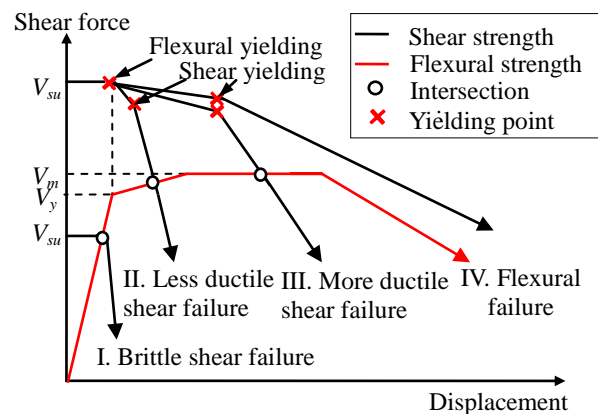


Fig.1 The conceptual failure modes

point is not reached the peak flexural strength (V_{mu}). When the flexural and shear strength intersects after the development of the peak flexural strength is reached, the ductile shear failure can be observed. In the case that the shear strength is higher than the flexural strength, columns perform as flexural failure in Mode IV.

In order to predict the shear strength of RC columns with and without FRP jacketing, the authors proposed a new analytical method which emphasizes on the interaction of flexural and shear strength. In the new method, the flexural strength is evaluated by the section analysis. This section analysis was combined with the shear strength mechanism, which was modeled based on the truss mechanism. The flexure-shear models showed significant interactions due to the reduction of reinforcement secant stiffness after yielding and concrete deterioration. The analytical method was verified using an experimental database with FRP-jacketing that was tested under reversed cyclic loading. The proposed analytical method is more effective for predicting the load-deformation relationship, including the post-peak behavior of

*1 Graduate student, Graduate School of Engineering, Hokkaido University, M.E, JCI Member

*2 Post-doctoral fellow, Faculty of Engineering, Hokkaido University, PhD. JCI Member

*3 Prof., Faculty of Engineering, Hokkaido University, Dr.E., JCI Member

FRP-jacketed RC columns, than the conventional analytical method and proves that fibers with high fracture strain can provide good ultimate ductility.

2. STRENGTH MODELS

2.1 Flexural Strength Model

To calculate the flexural strength of a column section, a section analysis [3] was performed by dividing the total depth of cross section (h) into a number of discrete strips as shown in Fig. 2. It was assumed that plane sections remain planes at any loading level. In the section analysis, the increments of strain in the compression at the top fiber (ε_{cc}) are given, and the strain across the depth of the cross-section is proportional to the distance through the neutral axis depth (x).

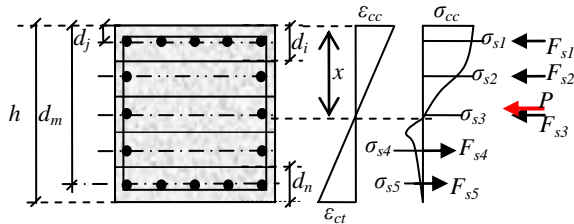


Fig.2 Section analysis

The enhancement of flexural strength appears in terms of confinement effect in the confined concrete stress-strain relationship. For a given flexural cross section, the force and moment equilibrium conditions are given as follows:

$$P = \sum_{i=1}^n \sigma_{ci} A_{ci} + \sum_{j=1}^m \sigma_{sj} A_{sj} \quad (1)$$

$$M = \sum_{i=1}^n \sigma_{ci} A_{ci} d_i + \sum_{j=1}^m \sigma_{sj} A_{sj} d_j \quad (2)$$

Therefore, the shear force corresponding to flexural strength (V_{mu}) can be obtained:

$$V_{mu} = \frac{M}{a} \quad (3)$$

where,

A : sectional area

V : volume

σ_{ci} = stress in i^{th} concrete layer = $\varepsilon_{ci} E_{ci}$

σ_{sj} = stress in j^{th} longitudinal reinforcement = $\varepsilon_{sj} E_{sj}$

d_i = distance from top fiber to the centroid of i^{th} concrete layer

d_j = distance from top fiber to the centroid of j^{th} steel reinforcement

A_{ci} = area of i^{th} concrete layer

A_{sj} = area of j^{th} longitudinal reinforcement

P = axial force

M = moment at the considered cross section

i, j = 1, 2, 3... n or m

a = shear span

As expressed in Fig. 2, the strain compatibility equations of the i^{th} concrete and the j^{th} longitudinal reinforcement are given in terms of the concrete strain at the top fiber (ε_{cc}) and at bottom fiber (ε_{ct}) as follows:

$$\varepsilon_{ci} = \varepsilon_{ct} + (\varepsilon_{cc} - \varepsilon_{ct}) \frac{h - d_i}{h} \quad (4)$$

$$\varepsilon_{sj} = \varepsilon_{ct} + (\varepsilon_{cc} - \varepsilon_{ct}) \frac{h - d_j}{h} \quad (5)$$

From the flexural strength model, the secant modulus of longitudinal reinforcement, shear reinforcement and concrete (E_{se} , E_{we} , E_{ce}), effective strength of concrete (f'_{ce}), concrete strain at the extreme fiber (ε_{cc}) and neutral axis depth (x) can be obtained. The secant modulus is calculated from the stress-strain relationship of corresponding materials. However, the neutral axis depth in the flexural strength model moves upward (Fig. 2) due to the shear crack deterioration depending on the shear strength model.

2.2 Shear Strength Model

Tidarut et al. [3] presented a shear strength model for RC beams which has verified its accuracy and reliability. In this study, this shear strength model is modified and extended to RC column by adding the effect of axial load due to the similarity of shear mechanism between RC beam and column. Previous experimental observations [1,6,7] showed that the shear strength of RC columns significantly relates to the secant stiffness of the flexural and shear reinforcements. Fig. 3 illustrates the shear strength model with influence of yielding when deformation increases.

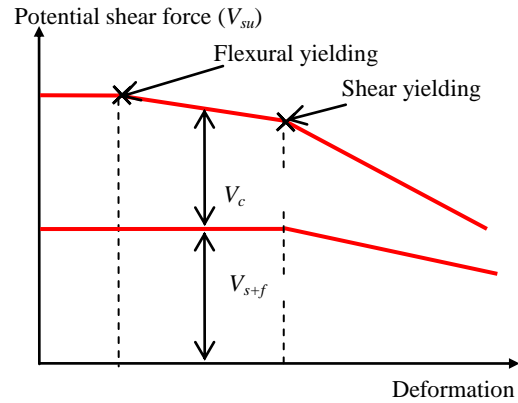


Fig.3 Shear strength model

In Fig. 3, when the flexural reinforcement reaches its yield strength, a reduction of the flexural stiffness occurs, and then a drop of potential shear capacity is observed. Moreover, the shear strength capacity continuously decreases after the yielding of the shear reinforcement because the shear reinforcement contribution has no further increase. The effective concrete strength (f'_{ce}) is another important parameter in the shear strength model. The effective concrete strength is considered as the remaining strength in the compressive softening region. As a result, the concrete resisting force decreases after the onset of the reduction of the effective concrete strength.

Fig. 4 depicts the truss mechanism proposed by Sato et al. [7]. It shows that after the formation of shear crack the resisting force due to compressive concrete (V_{cpz}) and aggregate interlocking (V_{str}) develop as the concrete shear strength (V_c). At the same time, the transverse shear strength due to steel and fiber reinforcement (V_s and V_f) develops to resist the further shear crack opening.

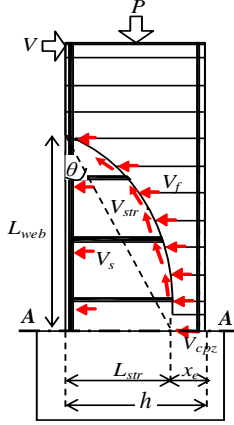


Fig.4 Truss mechanism (Sato et al.)

In RC columns, the total shear strength (V_{su}) is the summation of the contribution of the concrete (V_c) and the transverse reinforcement (V_{s+f}) as follows:

$$V_{su} = V_c + V_{s+f} \quad (6)$$

The concrete shear strength model (V_c) is considered from the experimental shear force component in the post-peak region. The concrete strength depends on five parameters; stiffness reduction of the flexural reinforcement ($\rho_s E_{se}$), the shear reinforcement ($\rho_w E_{we} + \rho_f E_{fe}$), the shear span-to-depth ratio (a/d), axial load ratio ($P/A_g f'_c$) and the effective concrete strength (f'_{ce}). Using a non-linear regression analysis, the concrete contribution to shear strength is proposed as follows:

$$V_c = \beta_d \cdot \beta_p \cdot \beta_s \cdot \beta_w \cdot f_{vcd} \cdot b \cdot d \quad (7)$$

where $f_{vcd} = 0.2 \sqrt[3]{f'_{ce}}$, $\beta_d = \sqrt[4]{a/d}$, $\beta_p = \sqrt{\frac{P}{2.5 A_g f'_c}}$,
 $\beta_s = \sqrt[4]{\rho_s E_{se}}$ and $\beta_w = \sqrt[4]{\rho_w E_{we} + \rho_f E_{fe}}$

Both the web and fiber reinforcement are assumed to resist the shear force monolithically and the model to predict this becomes a single term, V_{s+f} .

$$V_{s+f} = b L_{web} \bar{\varepsilon}_w (\rho_w E_{we} + \rho_f E_{fe}) \quad (8)$$

From the experimental data, it was found that average tensile strain of transverse reinforcement is affected by the same parameters proposed by Sato in his equation [7]. Utilizing a multiple non-linear regression analysis, an empirical formula is proposed to express the average strain of the transverse

reinforcement ($\bar{\varepsilon}_w$) where it is considered that fiber strain and steel tie strain have the same value.

$$\bar{\varepsilon}_w = 0.004 \frac{\sqrt{f'_{ce}}}{\sqrt{a/d} + 1} \left(e^{\rho_s E_{se}} - 0.12 \sqrt{\rho_w E_{we} + \rho_f E_{fe}} \right) \quad (9)$$

To estimate the size of concrete compression zone, the shear strength equations of cut plane (section A-A as expressed in Fig. 4) are developed [7]. The neutral axis depth, affected by various factors, becomes smaller in shear cracking zone (x_e) than that by the bending theory (x). Thus, the depth of compression zone is expressed as follows:

$$\frac{x_e}{x} = \left[\frac{1 - e^{-0.42 a/d}}{1 + 3.2 e^{-0.12 (\rho_w E_{we} + \rho_f E_{fe})^{0.4}}} \right] \left[1.25 e^{-0.08 \left(\frac{\rho_s E_{se}}{1000} \right)} \right] \quad (10)$$

where x is the neutral axis depth calculated by bending theory as follows:

$$x = d \left(-n \rho_s + \sqrt{(n \rho_s)^2 + 2 n \rho_s} \right) \quad (11)$$

where ρ_s , ρ_w and ρ_f denote the ratio of tension, web and fiber reinforcement respectively.

The vertical and horizontal projected lengths of the shear cracking region are L_{str} and L_{web} as shown in Fig.4, respectively. However, the angle of the diagonal shear crack (θ) is assumed as 45° [3], which is a conservative assumption. Thus, the actual angle is used to obtain the precise length of shear crack.

$$L_{str} = h - x_e \quad (12)$$

$$L_{web} = \frac{L_{str}}{\tan \theta} \quad (13)$$

It should be noted that the proposed shear strength model is applicable to the case of shear compression failure of linear members with shear reinforcement.

2.3. Flexure-Shear Interaction

Fig.5 presents the analytical procedure for the flexure-shear interaction method. The first step in the analytical procedure involves the given value of the strain of concrete at the top fiber, which is defined as ε_{cc} . The section analysis is performed by dividing the section into number of strips as previously explained in Fig.2. Applying the compatibility and force equilibrium conditions are satisfied, all parameters, secant modulus (E_{se}), remaining concrete stress (f'_{ce}), neutral axis depth (x) and flexural strength (V_{mu}) can be determined. Using these parameters, the shear strength model is considered based on the truss mechanism. Then, the neutral axis depth with shear crack effect (x_e) in the shear strength model is obtained and compared with the neutral axis depth from the section analysis (x). Then, the section analysis reanalyze by updating the neutral

axis depth obtained from the shear strength model. In the section analysis, the secant stiffness and concrete strength are recalculated based on the compatibility and equilibrium conditions through the iteration process. When the x -value reaches the x_e -value, the shear strength value (V_{su}) is obtained at the same time the deformation components are calculated. Finally, the load-deformation relationship can be drawn.

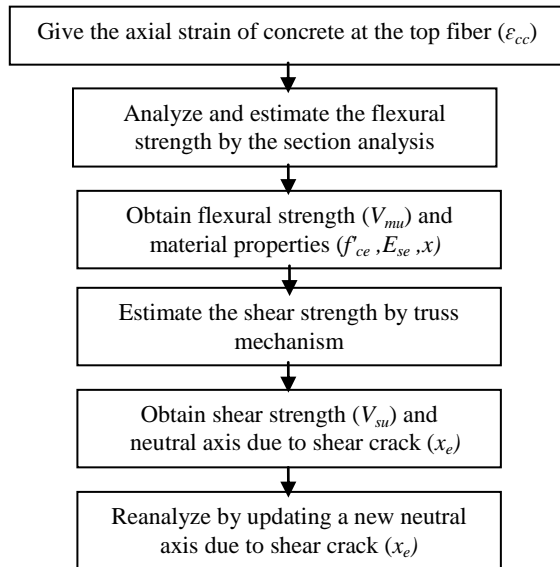


Fig.5 Flexure-shear interaction procedure

3. EXPERIMENTAL DATABASE

To evaluate shear strength degradation in post-peak region, the experimental database of 13 laboratory tests on reinforced concrete columns failing in both shear and flexure-shear were compiled. The details of database are summarized in Table 1.

Table 1 Database of column tests

Type	Fiber	f'_c MPa	ρ_s^{*1} %	ρ_w^{*2} %	ρ_f^{*3} %	P/A_g f'_c	Failure modes
SP1	-	29.5	2.87	0.16	0.00	0.03	BS
SP4	PET	29.5	2.87	0.16	0.37	0.03	DS
SP5	PET	31.7	2.87	0.16	0.19	0.03	DS
SP6	PET	31.7	2.87	0.16	0.12	0.03	DS
SP7	PET	31.7	2.87	0.16	0.06	0.03	DS
SP8	-	31.7	2.87	0.16	0.00	0.03	BS
SP9	PET	31.7	3.59	0.16	0.12	0.03	DS
SP10	PET	31.7	2.15	0.16	0.06	0.03	DS
AS-NS1	-	31.4	1.30	0.61	0.00	0.40	BS
ASC-NS2	CF	36.5	1.30	0.61	0.65	0.38	DS
ASC-NS3	CF	36.9	1.30	0.61	1.30	0.65	DS
ASC-NS4	CF	36.9	1.30	0.61	0.65	0.65	DS
ASC-NS5	CF	37.0	1.30	0.61	1.95	0.65	DS

*¹ tension steel ratio, *² web steel ratio, *³ fiber reinforcement ratio, BS= Brittle shear failure (Mode I), DS = Ductile shear failure after the peak flexural strength (V_{mu}) has reached (Mode III)

According to Anggawiddjaja's experiment [1], a total of thirteen square RC columns (denoted as SP) with various types of FRP jacket, PET fiber, were

collected. The cross-section of his column is 400x400 mm. For specimens SP1 and SP4, the shear span to the depth ratio (a/d) is equal to 3 while for specimens SP5-10 is 4. Iacobucci et al. [5] studied on reinforced concrete square columns lacking of web reinforcing steel to represent existing old columns designed based on an old seismic specification. His main focus is on testing columns with and without CFRP jacketing under lateral cyclic displacement and high axial load ratio ($P/A_g f'_c$). His columns are denoted as AS and ASC with 305x305mm in cross-section dimension. The fiber configuration of all databases was oriented perpendicular to the longitudinal axis of the column or in the shear direction and all retrofitted columns were fully wrapped by FRP sheet.

4. MODEL VERIFICATION AND ANALYTICAL RESULTS

The experimental results of FRP shear-strengthened RC columns failing in brittle shear and ductile shear [1,5] were selected to verify the applicability of the proposed shear strength model in the post-peak region where the shear strength is dominant. Moreover, the analytical results of load-deformation relationships are compared with that of experimental results in order to verify the accuracy of the new analytical method accounting for flexure-shear interaction.

4.1 Comparison of Calculated and Measured Concrete Contribution

Fig. 6 shows the comparison between calculated and experimental concrete shear strength. The concrete shear strength from experiment ($V_{c-experiment}$) is calculated by subtracting V_{s+f} from V_{total} . The V_{s+f} value is obtained from the strain gauge which is mounted on the steel and fiber reinforcement. Good estimation between concrete strength from experiment and proposed model can be achieved.

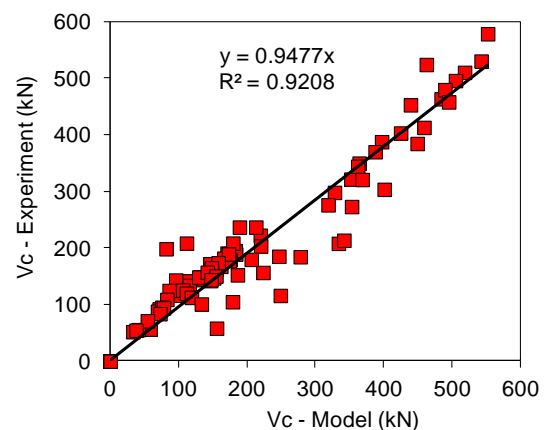


Fig.6 Vc Experiment and Vc Model

4.2 Comparison of Calculated and Measured Transverse Reinforcement Contribution

In Fig. 7, the shear strength carried by steel and fiber reinforcement obtained from the model agree well with the experimental results.

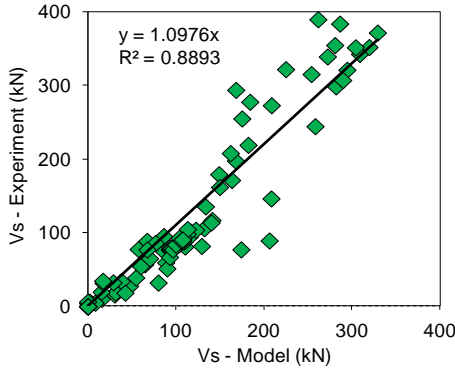


Fig.7 Vs Experiment and Vs Model

4.3 Load-deformation relationships

For simplicity, analytical and experimental load-deformation relationships under reversed cyclic loading were described as an enveloped curve. In order to predict the load-deformation relationship, the strength and deformation models were computed by a numerical procedure. Fig. 8 illustrates the load-deformation relationships from the experiment tested by Anggawiddjaja et al. and from the analytical method. For specimens SP1 and SP4, load-deformation relationships are expressed in Fig. 8 (a).

For the specimens SP5-10, the effects of the fiber volumetric ratio (ρ_f) and the shear strength ratio (ρ_w) on the improvement of strength and ductility were considered as shown in Figs. 8 (b)-(f). A sudden decrease in load carrying capacity was observed in specimen SP8 (controlled specimen) because concrete strength reduction due to compression softening,

spall-off and reduction of reinforcement stiffness occurred simultaneously. However, specimens jacketed by PET fiber (SP5, SP6, SP7, SP9, SP10) showed higher in both load carrying capacity and ductility. This indicates that PET fiber is less likely to fracture before a concrete column reaches its ultimate deformation.

Regarding the fiber breakage, the tested outcomes of specimens SP7 and SP10 showed the breakage of fiber in the post-peak region. The rupture of the fiber according to the analytical program began at the same time as that of experiment. However, slightly conservative breakage point can be observed in specimen SP9. This shows that the analytical method can also accurately predict fiber rupture, and the analytical results agreed well with experimental results.

Fig. 9 demonstrates the load-deformation relationships from the experiment tested by Iacobucci et al. and from the analytical method. The load-carrying capacity of specimen AS-NS1 failing in brittle shear suddenly dropped due to concrete spall off and less confinement of transverse reinforcement. The analytical tool overestimated post-peak load-deformation behavior since in the calculation the overestimation of the shear strength can be observed. Moreover, the concrete strength is assumed to carry 20% of compressive strength in the softening concrete model which in fact the cover concrete cannot carry load after its spall-off. To examine the influence of fiber ratio to the shear strength and ductility, the retrofitted columns ASC-NS1-5 were analyzed and it can be seen that the analytical method can predict the post-peak behavior of these retrofitted column well.

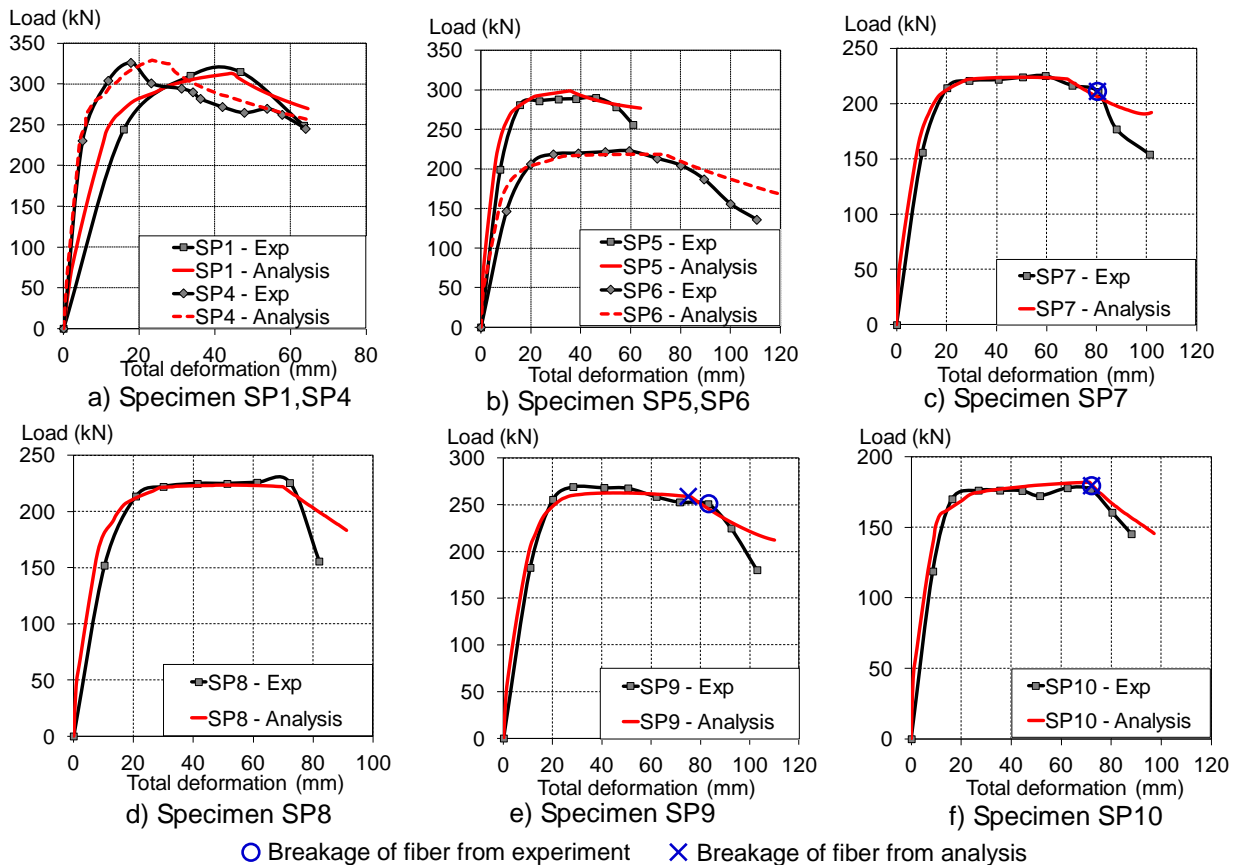


Fig. 8 Load-deformation relationships of database tested by Anggawiddjaja et al.

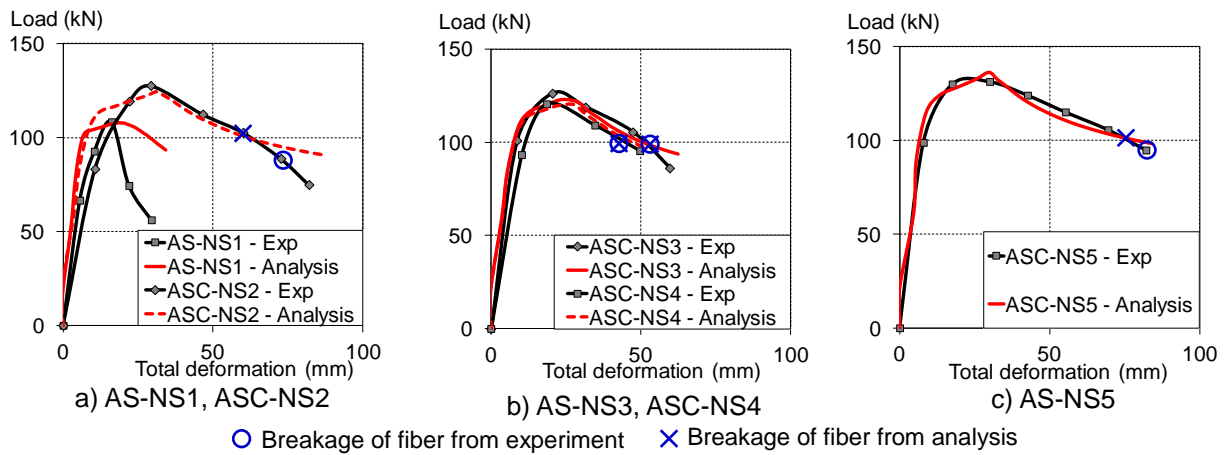


Fig. 9 Load-deformation relationships of database tested by Richard et al.

The overall load-deformation relationships from the experiment agreed well with the analytical predictions in terms of both strengths and deformations. In addition, the specimens that were retrofitted by high fracture strain but low stiffness (PET) such as SP4 showed an enhancement in ductility. Therefore, it is proven that the FSI analytical method is applicable for not only FRP with high fracture strain (PET) but also FRP with low fracture strain (CFRP). In summary, the flexure-shear interaction analytical method improves the prediction of the load-deformation relationships of RC columns with and without FRP-jacketing when compared to the conventional section analysis.

5. CONCLUSIONS

This paper presented an analytical method taking into account the interaction of flexural and shear strength models. Using section analysis, the flexural strength can be evaluated. Meanwhile, the proposed shear strength model considering several parameters such as the effect of fiber confinement, secant stiffness of reinforcement, tension reinforcement ratio, fiber ratio, shear span to depth ratio and concrete strength. Experimental database of 13 RC columns with and without FRP-jacketing were compiled to verify the applicability and reliability of the analytical method. The conclusion of this research study is as follows:

- (1) The flexure-shear interaction analytical method can successfully predict the load-deformation relationships of RC columns with and without FRP retrofitting.
- (2) The flexural strength model connects with the shear strength model by the neutral axis depth of the shear crack region, whereas the shear strength model connects with the flexural strength model by the yielding of reinforcement. The proposed model can predict well the shear strength components carried by shear reinforcement, such as steel reinforcement and FRP jacket.
- (3) The proposed shear strength model can predict the shear strength of reinforced concrete columns with and without PET-fiber jacketing in the post-peak

region. The experimental results are well correlated with the proposed predictive model.

ACKNOWLEDGEMENT

The authors would like to acknowledge Mr Hiroshi Nakai of Maeda Kosen Co. Ltd, Japan and the Aramid Reinforcement Association for providing epoxy resin and PET fiber for providing invaluable advice and support towards this research study.

REFERENCES

- [1] Anggawidjaja, D., Ueda, T., Dai, J., and Nakai, H.: "Deformation capacity of RC piers wrapped by new fiber-reinforced polymer with large fracture strain," *Cement and Concrete Composites*, Vol.28, No. 10, 2006, pp. 914-927
- [2] Japan Society of Civil Engineers (JSCE): "Recommendations for upgrading of concrete structures with use of continuous fiber sheets," *Concrete engineering series 41*, 2001, pp. 250
- [3] Jirawattanasomkul, T., Ikoma, Y., Zhang D., and Ueda, T.: "Shear Strength of Reinforced Concrete Members Strengthened with FRP Jacketing," *Japan Concrete Institute, Proceedings of the Annual Convention of Japan Concrete Institute*, Osaka, Japan, Vol.33, No.2, 2011, pp.991-996
- [4] Jirawattanasomkul, J., Anggawidjaja, D. and Ueda, T.: "Seismic Retrofitting by FRP Jacketing and Prediction Method of Ultimate Deformation," *CICE - The 5th International Conference on FRP Composites in Civil Engineering*, Vol. 2, 2010, pp.806-809
- [5] Iacobucci, R. D., Sheikh, S. A. and Bayrak, O.: "Retrofit of Square Concrete Columns with Carbon Fiber-Reinforced Polymer for Seismic Resistance," *ASCE Journal of Structural Engineering*, Vol.100, No.6, 2003, pp.785-794
- [6] Priestley, M. J., Verma, R., and Xiao, Y.: "Seismic Shear Strength of Reinforced Concrete Columns," *ACI Struct. J.*, Vol.120, No.8, 1994, pp.218-226
- [7] Sato, Y., Ueda, T., and Kakuta, Y.: "Shear Strength of Prestressed Concrete Beams with FRP Tendon," *JSCE*, Vol. 28, No.27, 1995, pp. 189-208